

E11-2023-37

A. M. Chervyakov*

ON FINITE-ELEMENT MODELING
OF LARGE-SCALE MAGNETIZATION PROBLEMS
WITH COMBINED MAGNETIC VECTOR
AND SCALAR POTENTIALS

Submitted to “Physics of Particles and Nuclei Letters”

* E-mail: acher@jinr.ru

Червяков А. М.

E11-2023-37

О конечно-элементном моделировании в задачах магнитостатики на основе совместного использования магнитных векторного и полного скалярного потенциалов

Для эффективного решения ресурсно-затратных задач магнитостатики проводится анализ численной эффективности конечно-элементного моделирования на основе совместного использования векторного и полного скалярного магнитных потенциалов. Потенциалы определяются уравнениями Максвелла для проводящих и непроводящих областей решаемой задачи и условиями сопряжения на общей границе раздела. Для корректности комбинированной формулировки в непроводящих областях строятся разрезы, обеспечивающие их односвязность. В качестве иллюстрации используются модели катушки Гельмгольца и дипольного магнита. По сравнению с формулировкой, использующей только векторный потенциал, применение комбинированной формулировки позволяет добиться значительного сокращения как объёма компьютерной памяти, так и времени вычислений при аналогичной точности обоих методов.

Работа выполнена в Лаборатории информационных технологий им. М. Г. Мещерякова ОИЯИ.

Препринт Объединенного института ядерных исследований. Дубна, 2023

Chervyakov A. M.

E11-2023-37

On Finite-Element Modeling of Large-Scale Magnetization Problems with Combined Magnetic Vector and Scalar Potentials

A numerical performance of finite-element modeling based on the combination of magnetic vector and total scalar potentials is assessed against the vector potential formulation for two magnetization problems, the Helmholtz coil and the dipole magnet. The potentials are applied to conducting and nonconducting parts of the problem domain and coupled together across their common interfacing boundary. Thin cuts are constructed in the current-free regions to ensure the consistency of the formulation. Simulation results show a substantial reduction in the computational cost provided by the mixed formulation compared to its vector counterpart for a similar accuracy of both methods.

The investigation has been performed at the Meshcheryakov Laboratory of Information Technologies, JINR.

Preprint of the Joint Institute for Nuclear Research. Dubna, 2023

INTRODUCTION

Finite-element method (FEM) simulations of large-scale 3D magnetostatic problems such as the magnetization of magnets can be computationally expensive due to complexity of geometries separated by differing media, nonlinearity of involved materials and enhanced requirements for accuracy of computations [1–4]. The solution of such problems is therefore limited by the available hardware resources. In particular, the capacity of the random-access memory (RAM) is crucially affected by direct solvers despite their out-of-core mechanism of distributing memory, while the CPU-processing time is considerably elongated by iterative solvers. A common tool for FEM calculation of the magnetostatic fields in the presence of currents and nonlinear materials is based on the magnetic vector potential (MVP) formulation [5–7]. Although this approach provides a superior quality of calculations, exploiting the vector potential for entire problem domain including large current-free regions increases the total number of the model degrees of freedom (DOFs) and, therefore, the usage of computational memory and time. In order to reduce the computational cost, the regions that are free from the currents can be modeled instead with magnetic scalar potential (MSP), while leaving the current-carrying regions for the use of magnetic vector potential and coupling both potentials on their common interfacing boundaries. However, such a combination of vector and scalar potentials when applied to conducting and nonconducting regions of the problem domain, respectively, must be consistent with Ampere’s law unless the nonconducting regions are made simply connected in the presence of currents. A typical example is provided by the geometry of a circular coil surrounded by a large insulating region of air in which the magnetic scalar potential is initially multivalued. There are several ways to overcome such a contradiction, the simplest being to extend the vector potential region to the hole area which is a part of the insulator. However, the most effective method, discussed in this paper, consists of constructing the thin cuts to prevent all paths from linking the currents and imposing across each cut surface the potential jump equal to the enclosed current [8–11]. Although creating the cuts may not be quite simple for nontrivial model geometries, it allows for substantial reduction in the computational cost. Moreover, for some problems, the application of the total scalar potential can be extended to the whole computational domain

where the exciting currents are represented as the line currents flowing along the cut boundaries [12, 13]. In this paper, the numerical potential of the mixed formulation is evaluated for two modeling examples, the Helmholtz coil surrounded by air and the dipole magnet, and compared with the potential of the MVP formulation. We show that the use of the mixed formulation results in substantial reduction of computational expenses while keeping almost the same quality of numerical computation.

1. MODELING FRAMEWORK

1.1. Magnetostatic Equations. In magnetostatics (see, e.g., [14]), the fields caused by steady currents are described as a static limit of Maxwell's equations given by magnetic Gauss's and Ampere's laws explicitly as

$$\nabla \times \mathbf{H} = \mathbf{j}, \quad \text{in } \Omega, \quad (1)$$

$$\nabla \cdot \mathbf{B} = 0, \quad \text{in } \Omega, \quad (2)$$

where bold letters are referred to three-component vectors, \mathbf{j} is a divergence-free ($\nabla \cdot \mathbf{j} = 0$) source current density, \mathbf{B} and \mathbf{H} are the magnetic flux density and magnetic field strength, respectively. They are further related to each other via the constitutive relation accounting for macroscopic properties of the materials

$$\mathbf{B} = \mu \mathbf{H}, \quad \text{in } \Omega, \quad (3)$$

with μ being the permeability of medium. Most of the magnetostatic problems involve several materials of different permeabilities including those with highly nonlinear behavior of the corresponding magnetization curves $\mu(H)$. For such problems, μ is continuous within a material and discontinuous across the material interfaces.

Equations (1)–(3) hold for the whole problem domain Ω , ensuring simultaneously the continuity of the tangential component of the vector \mathbf{H} (with no surface currents) and the normal component of the vector \mathbf{B} on its boundary $\Gamma = \partial\Omega$:

$$\mathbf{n} \times \mathbf{H} = 0, \quad \text{on } \Gamma_h, \quad (4)$$

$$\mathbf{n} \cdot \mathbf{B} = 0, \quad \text{on } \Gamma_b, \quad (5)$$

where Γ_h and Γ_b are the two complementary parts of entire boundary $\Gamma = \Gamma_h \cup \Gamma_b$ distinguished in accordance with antisymmetry/symmetry conditions (also known as the perfect magnetic conductor/the magnetic insulation conditions), respectively. The boundary conditions (4) and (5) are imposed to truncate/magnetically insulate the whole model geometry. They can also be used as interface conditions separating different media.

Given relation (3), Eqs. (1) and (2) form a first-order div-curl system of four scalar equations in three unknowns. In principle, FEM analysis of such a system, e. g., in terms of the flux density \mathbf{B} , can be done by using the least squares method (LSFEM) with residuals including both Eqs. (1) and (2) and the boundary condition (5) as well. However, the LSFEM does not work well

for the problems with abrupt changes in material coefficients [15]. A standard approach is therefore to formulate the problem in terms of potentials rather than in primary field variables. Depending on the problem objectives, the fields can be expressed either by the magnetic scalar potential, or by the magnetic vector potential considered as new dependent variables. The MSP formulation obviously requires less degrees of freedom than the MVP formulation for finite element modeling, but may be mathematically more elaborated in the presence of currents. In order to reduce the total number of DOFs and increase the efficiency of computation, it is also possible to use the combined formulation applying one of the potentials to a certain region of the problem domain. The comparative analysis of using these formulations is presented below.

1.2. The MSP Formulation. Introduction of the magnetic scalar potential V_m originally begins with the regions without currents ($\mathbf{j} = 0$), where according to Eq. (1), the magnetic field \mathbf{H} becomes purely irrotational, and therefore can be represented as a negative gradient of the scalar potential $\mathbf{H} = -\nabla V_m$ to satisfy Ampere's law identically. In terms of the scalar potential, the magnetic Gauss's law (2) is then described with the help of the constitutive relation (3) by Laplace's equation explicitly as

$$\nabla \cdot (\mu \nabla V_m) = 0, \quad \text{in } \Omega, \quad (6)$$

where the permeability μ reads as

$$\mu(H) = B(H)/H, \quad \text{in } \Omega, \quad (7)$$

and $B(H)$ is a material-dependent magnetization curve. The corresponding to (4) and (5) boundary conditions take the following form:

$$V_m = 0, \quad \text{on } \Gamma_h, \quad (8)$$

$$\mathbf{n} \cdot \nabla V_m = 0, \quad \text{on } \Gamma_b. \quad (9)$$

The zero magnetic scalar potential boundary condition (8) (or, the antisymmetry condition) enforces the continuity of scalar potential across the interface of different media preserving simultaneously the uniqueness of its definition. Indeed, although the potential can be uniquely defined at one reference point chosen arbitrarily somewhere in any part of the problem domain, this choice should be common for all other adjacent parts of such domain, that is along the common boundary interface what is exactly stated by Eq. (8), where the zero scalar potential point is specified.

When currents are involved in the problem domain, the scalar potential becomes undefined in conducting regions and multivalued in nonconducting regions if they are multiply connected [9–11]. One way to cope with the second problem is to construct the thin cuts preventing any closed path from linking the currents and impose the potential discontinuity across different sides of each cut surface as follows:

$$\Delta V_m = V_m^+ - V_m^- = I, \quad \text{on } \Gamma_{\text{cut}}. \quad (10)$$

Equation (10) ensures that the induced in a nonconducting region magnetic field corresponds to the exciting current flowing in a conducting loop. On finite element basis, the scalar potential is approximated by Lagrange nodal elements with DOFs specified by its value at each node. These nodes are then duplicated on the cut surfaces to distinguish between the two sides of each surface and constrain the potential difference according to Eq. (10). In this way, the scalar potential becomes a single-valued function everywhere in nonconducting regions surrounding currents as far as they are made simply connected. The first problem is then resolved either via introducing the magnetic vector potential for conducting regions and using the mixed vector-scalar formulation for the whole problem domain, where both potentials are coupled together across common interfaces, or by representing the exciting currents as the line currents flowing along the cut boundaries, whose values are accounted for by the potential discontinuities, extending thereby the MSP formulation to the entire problem domain.

Multiplying Eq. (6) by a scalar test function ζ with the boundary condition ($\zeta = 0$ on Γ_h), integrating by parts over the computational domain Ω and using boundary condition (9), we obtain the weak formulation in terms of scalar potential

$$\int_{\Omega} (\mu \nabla V_m) \cdot (\nabla \zeta) dv - \int_{\Gamma_{\text{cut}}} \mu \zeta \mathbf{n} \cdot (\nabla V_m^+ - \nabla V_m^-) ds = 0, \quad (11)$$

where Γ_{cut} is a cut surface, while the function ζ after discretizing on a finite-element mesh represents a set of nodal basis functions ζ_i used to approximate the scalar potential V_m following the Galerkin method. In the presence of several cuts, the last term in (11) is extended to the sum over all cut surfaces.

1.3. The MVP Formulation. The number of Eqs. (1) and (2) can also be reduced by accounting for solenoidality of the magnetic flux density \mathbf{B} and introducing the magnetic vector potential \mathbf{A} as $\mathbf{B} = \nabla \times \mathbf{A}$. This satisfies identically Eq. (2) describing Gauss's law, while Eq. (1) for Ampere's law takes the form of a double curl equation

$$\nabla \times \left(\frac{1}{\mu} \nabla \times \mathbf{A} \right) = \mathbf{j}, \quad \text{in } \Omega, \quad (12)$$

where the permeability μ is now expressed as

$$\mu(B) = B/H(B), \quad \text{in } \Omega, \quad (13)$$

and $H(B)$ is a magnetization curve specified for each material. In terms of vector potential, the corresponding to (4) and (5) boundary conditions read, respectively, as

$$\mathbf{n} \times \nabla \times \mathbf{A} = \mathbf{0}, \quad \text{on } \Gamma_h, \quad (14)$$

$$\mathbf{n} \times \mathbf{A} = \mathbf{0}, \quad \text{on } \Gamma_b, \quad (15)$$

where the magnetic insulation boundary condition (15) (or, the symmetry condition) enforces the tangential continuity of the potential \mathbf{A} across the boundary and follows directly from its definition.

The vector potential is not uniquely defined unless its divergence is specified. Without gauge fixing, the numerical modeling in three dimensions would be faced with instabilities and/or singularities of the algebraic system corresponding to Eq.(12). In fact, the nontrivial null space of the curl-curl operator in Eq.(12) involving the gradient of an arbitrary scalar field appears due to gauge freedom in the definition of the magnetic vector potential [16, 17]. However, despite the ambiguity of the potential, the magnetic field and the flux density are always uniquely calculated by its means. Moreover, when only these physical quantities are matters of interest, the singular algebraic system for unknown potential can be handled by iterative solvers due to their inherent auto-gauging properties.

On the other hand, the gauge fixing might be necessary when either the uniqueness of solution for unknown potential is required, or the only direct solvers are available for its numerical computation [18]. As the MVP formulation relies merely on the curl of the vector potential, its divergence can be chosen arbitrarily. A common choice corresponds to the Coulomb gauge

$$\nabla \cdot \mathbf{A} = 0, \quad \text{in } \Omega. \quad (16)$$

Once imposed, the gauge (16) would result in yet another boundary condition

$$\mathbf{n} \cdot \mathbf{A} = 0, \quad \text{on } \Gamma_h \quad (17)$$

implying the normal continuity of the magnetic vector potential across the boundary. By Eqs.(15) and (17), the gauged \mathbf{A} field becomes continuous in both the tangential and the normal directions to the boundary surface. Although such a continuity can be preset automatically by the approximation of the potential \mathbf{A} on the nodal finite-element basis with its three components specified at each node, this would not be done without loss of accuracy for the problems with discontinuous medium properties, where the normal component of the potential is changed abruptly at material interfaces [6]. In modeling such problems, the common approach is therefore to approximate the vector potential with only tangential component continuous while leaving its normal component free to jump across the boundary by using instead of nodal the edge (curl-conforming) elements with DOFs assigned in a finite-element mesh along each edge rather than at each node [19, 20].

The edge elements are not divergence-free in general to enforce the Coulomb gauge (16) automatically on the finite-element basis [19]. This gauge is therefore imposed in a weak form via introducing a Lagrange multiplier ψ as a new dependent variable [20–23]. Applying ψ to Ampere’s law results in two coupled equations: one for the multiplier ψ given by condition (16) and the other for the potential \mathbf{A} expressed by the modified double curl equation

as compared to (12) as follows:

$$\nabla \times \left(\frac{1}{\mu} \nabla \times \mathbf{A} \right) = \mathbf{j} + \nabla \psi, \quad \text{in } \Omega, \quad (18)$$

where the value of variable ψ is set to a constant on insulation boundaries to avoid possible singularities.

The weak formulation in terms of magnetic vector potential is based on Eqs. (16)–(18). Simplest, Eqs. (16) and (17) are represented by the following integral equation:

$$\int_{\Omega} \mathbf{A} \cdot (\nabla \zeta) \, dv = 0, \quad (19)$$

where ζ is a scalar test function satisfying the boundary condition ($\zeta = 0$ on Γ_b). The weak form of Eq. (18) is then obtained multiplying (18) by the vectorial test function \mathbf{w} with the boundary condition ($\mathbf{n} \times \mathbf{w} = 0$, on Γ_b), integrating by parts over the computational domain Ω and using boundary condition (14) explicitly as

$$\int_{\Omega} \left(\frac{1}{\mu} \nabla \times \mathbf{A} \right) \cdot (\nabla \times \mathbf{w}) \, dv = \int_{\Omega} \mathbf{j} \cdot \mathbf{w} \, dv + \int_{\Omega} (\nabla \psi) \cdot \mathbf{w} \, dv, \quad (20)$$

where \mathbf{w} is discretized on a finite-element mesh to represent a basis of the edge functions \mathbf{w}_i used for approximation of the potential \mathbf{A} following the Galerkin method. Equations (19) and (20) form a system of two coupled integral equations possessing unique solvability [20–23]. Aside from the gauge fixing, this system uses a gradient of ψ to eliminate any divergence from the externally applied current density \mathbf{j} , thereby ensuring the current continuity inherent in Ampere’s law. This would preserve the conservation of current in numerical calculation which is fulfilled automatically in the analytical sense but not obviously satisfied when interpolated on the finite-element functional basis.

1.4. The Mixed Formulation. A typical computational domain of the magnetostatic problems consists of the current-carrying region surrounded by the air and other nonconducting domains. Such a geometry suggests introducing the so-called mixed vector-scalar formulation solving Eqs. (1)–(5) for magnetic vector potential \mathbf{A} in the regions involving currents and for total scalar potential V_m in the current-free regions. As will be shown later, this leads to a substantial reduction in the computational cost. In the presence of currents, however, the magnetic scalar potential would only be consistently applied to current-free regions if they are simply connected meaning that no Ampere’s loops enclosing the current-carrying region are allowed there. Otherwise, the line integral of the magnetic field along a path enclosing the current would be equal either to zero, since the field is a gradient of the scalar potential, or to the value of the enclosed current due to Ampere’s law. As the scalar potential is assumed to be a single-valued function, such paths cannot be allowed. Typical geometries in which the scalar potential

regions are not simply connected are those that surround the vector potential regions possessing the holes. To make them simply connected, it is sufficient to prevent any closed path from linking a current by constructing the cut surfaces spanning the current-carrying regions. Simultaneously, this imposes the potential discontinuity across two different sides of each cut surface equal to the value of the enclosed current. In this way, the scalar potential becomes a single-valued function encountering, however, the jumps across each cut surface. On the finite-element basis, the vector potential is approximated by edge elements with DOFs specified by its tangential component along each edge, while the scalar potential is approximated by Lagrange nodal elements with DOFs specified by its value at each node. The conversion from nodal to edge elements can be performed [24].

The two potentials should be coupled on their common interfacing boundaries. The corresponding interface conditions follow directly from Eqs. (4) and (5) and guarantee the continuity of the tangential component of the field \mathbf{H} as well as the normal component of the flux \mathbf{B} . Equation (4) is used to specify the vector potential in terms of scalar potential, while Eq. (5) — to specify the scalar potential in terms of vector potential, so that the resulting conditions expressed by means of these potentials at an interfacing boundary between the MVP and MSP regions read as

$$\left(\frac{1}{\mu_c}\right) \cdot \mathbf{n} \times (\nabla \times \mathbf{A}) = -\mathbf{n} \times \nabla \cdot V_m, \quad \text{on } \Gamma_i, \quad (21)$$

$$-\mu_n \cdot \mathbf{n} \cdot \nabla \cdot V_m = \mathbf{n} \cdot (\nabla \times \mathbf{A}), \quad \text{on } \Gamma_i, \quad (22)$$

where Γ_i is a common interfacing boundary, while subscripts c and n refer to conducting and nonconducting regions, respectively. Note that the normal component of the curl of \mathbf{A} in the right-hand side of Eq. (22) is completely defined by the tangential component of \mathbf{A} .

The weak form of the mixed vector-scalar formulation is essentially based on Eqs. (19) and (20) applied to conducting domain Ω_c as well as on Eq. (11) for nonconducting domain Ω_n which are used together with conditions (21) and (22) preliminary expressed in a weak form. This yields the system of coupled integral equations for the mixed vector-scalar formulation as follows:

$$\int_{\Omega_c} \left(\frac{1}{\mu_c} \nabla \times \mathbf{A}\right) \cdot (\nabla \times \mathbf{w}) dv - \int_{\Gamma_i} (\mu_n \mathbf{n} \times \nabla V_m) \cdot \mathbf{w} ds = \int_{\Omega_c} \mathbf{j} \cdot \mathbf{w} dv + \int_{\Omega_c} (\nabla \psi) \cdot \mathbf{w} dv, \quad (23)$$

$$\int_{\Omega_n} (\mu \nabla V_m) \cdot (\nabla \zeta) dv + \int_{\Gamma_i} \mathbf{n} \cdot (\nabla \times \mathbf{A}) \zeta ds - \int_{\Gamma_{\text{cut}}} \mu \zeta \mathbf{n} \cdot (\nabla V_m^+ - \nabla V_m^-) ds = 0, \quad (24)$$

$$\int_{\Omega_c} \mathbf{A} \cdot (\nabla \zeta) dv = 0. \quad (25)$$

Some analytical results regarding to ellipticity of the bilinear form as well as the uniqueness of solution for such type of systems can be found elsewhere [20–23]. Next steps toward finding the numerical solutions such as meshing the computational domain with small nonoverlapping elements, approximating the unknown vector and scalar potentials on a finite-element mesh by the local edge and nodal basis functions, respectively, as well as discretizing the weak forms of PDEs to build up the local matrices, assembling the local matrices to a global matrix and, finally, solving linear algebraic systems are performed with COMSOL Multiphysics software specially adjusted to obtain the stable solutions.

It should be noted that the mixed vector-scalar formulation has been already implemented in the *Rotating Machinery, Magnetic* interface of COMSOL Multiphysics, specifically designed for modeling the magnetic rotating machines [25]. In particular, the interface uses the moving mesh approach to enable the relative motion of stators and rotors. To be meshed separately, these two parts must be treated as separated geometrical objects combined into an assembly pair with the prescribed rotor–stator coupling. Although it is possible, the application of this interface for modeling of stationary magnets would lead, however, to the unnecessary complexity.

In this paper, we employ instead the two other interfaces of this software, the *Magnetic Fields* and the *Magnetic Fields, No Currents*, usually used separately to solve either for magnetic vector, or for total scalar potential. We implement the mixed formulation by manually coupling these interfaces to each other along their common interfacing boundary to solve for combination of both potentials.

2. MODELING EXAMPLES

2.1. Models and Modeling Approaches. In order to evaluate the numerical potential of the mixed vector-scalar formulation against the MVP formulation, we use two magnetization models — the Helmholtz coil surrounded by air and the dipole magnet (Fig. 1).

The Helmholtz Coil Carrying DC Current. The model consists of two circular coils arranged in parallel at equal distances above and below the median plane of the large spherical air domain used for magnetic insulation. There are no nonlinear materials in this model.

Dipole Magnet. The model consists of two poles arranged in parallel at equal distances above and below the median plane of the large spherical air domain used for magnetic insulation. Either pole of the magnet includes the circular coil driven by DC current as well as the yoke, four spiral sectors and other constituents made of the nonlinear ferromagnetic materials.

The geometry of circular coil is identical for both models. It represents the axisymmetric hollow cylinder formed by rotation around the z axis of a rectangle lying in the (z, x) plane. The coil is of the multiturn type and therefore modeled as a homogenized current-carrying region with multiple

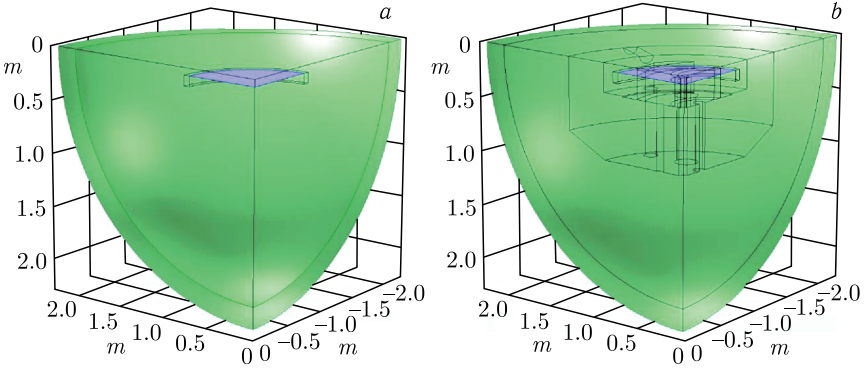


Fig. 1. The 1/8-th parts of the model geometries of the Helmholtz coil (a) and dipole magnet (b) surrounded by the insulation air domain with constructed cut surfaces

wires arranged and placed in a potting material. The excitation DC current of the same value for both models is applied to the coil internal cross-section boundary. A coil numeric analysis is made prior to the field calculation to compute the magnitude and direction of the current flow in a conductor. The coil current densities are shown in Fig. 2.

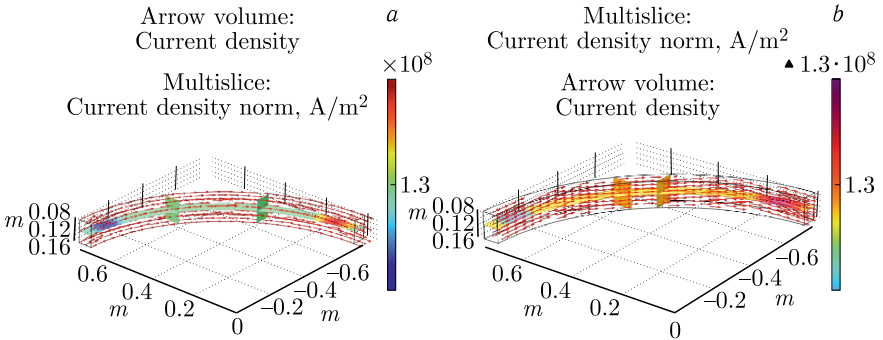


Fig. 2. The applied coil current densities in the models of the Helmholtz coil (a) and dipole magnet (b)

The geometry of the insulation air domain is also identical for both models. It represents a large sphere surrounded by the boundary layer, whose thickness is scaled towards infinity to mimic virtually the infinite element domain. Additionally, a single cut surface is constructed and added to geometries of both models when the mixed vector-scalar formulation is applied. Since the size and position of this surface do not affect the physics, the minimal area criterium is used for optimal construction providing the lower increase of the total number of DOFs after nodal doubling on the cut surface.

Both models possess three planes of symmetry allowing us to truncate the whole problem domain and reduce the computational cost by exploring the 1/8-th part of the model geometry and obtaining the results for the whole model. The mirror symmetry allows cutting the model geometries along the median plane and imposing either the Perfect Magnetic Conductor boundary condition (MVP formulation), or the Zero Magnetic Scalar Potential boundary condition (mixed formulation), whereas the four-fold axial symmetry is used to cut the remaining parts of the model geometries along the (z, x) and (z, y) planes and impose the Magnetic Insulation boundary conditions. The role of these boundary conditions is to mimic the entire geometry while exploiting its 1/8-th part.

In the MVP formulation, the magnetic vector potential is applied to the whole computational domain of both models. However, in the mixed formulation, the vector potential is only applied to the region of coil while the air and other nonconducting regions are modeled with the magnetic scalar potential. Both potentials are then coupled along the coil boundary by applying interface conditions (21) and (22) to ensure the field continuity.

The two studies relied on the same model geometry of both examples are performed and compared. The first study focuses on the numerical performance of the mixed vector-scalar formulation. The second one repeats a similar simulation by using the magnetic vector potential formulation. The main quantities of interest are the field distributions over the median plane as well as along the radial and azimuthal directions in the aperture area. For the FEM analysis of each model, the conforming mesh is generated with almost the same number of finite elements for different potential formulations despite the additional cut surface is constructed and added to geometries of both models when the mixed formulation is used. The minimal mesh quality is optimized to ensure the convergence and stability of solutions. The edge and Lagrange shape functions up to the third order are used for approximation of magnetic vector and scalar potentials, respectively. The mixed vector-scalar formulation is solved in fully coupled approach with the same for both potentials direct PARDISO solver based on multifrontal factorization of the stiffness matrix to ensure the convergence of solution. For the purpose of comparison, the same solver is then employed for the MVP formulation of both models. The gauge fixing for \mathbf{A} field is used with the direct solver as the necessary condition to ensure the convergence of solution. Its side impact on the convergence of nonlinear solver in the presence of the nonlinear materials for model of dipole magnet is overcome by splitting the solution process into several steps, each with its own behavior of the permeability specified as a constant, linear, and nonlinear, respectively, and with the initial conditions resulting from simulation of the previous step.

In the mixed formulation, the magnetic field outside the coil region of both models is obtained first by solving for the magnetic scalar potential and then taking the negative gradient from the solution result. For this reason, the potential discontinuities across the cut surfaces do not violate the continuity of the magnetic field as demonstrated in Fig. 3.

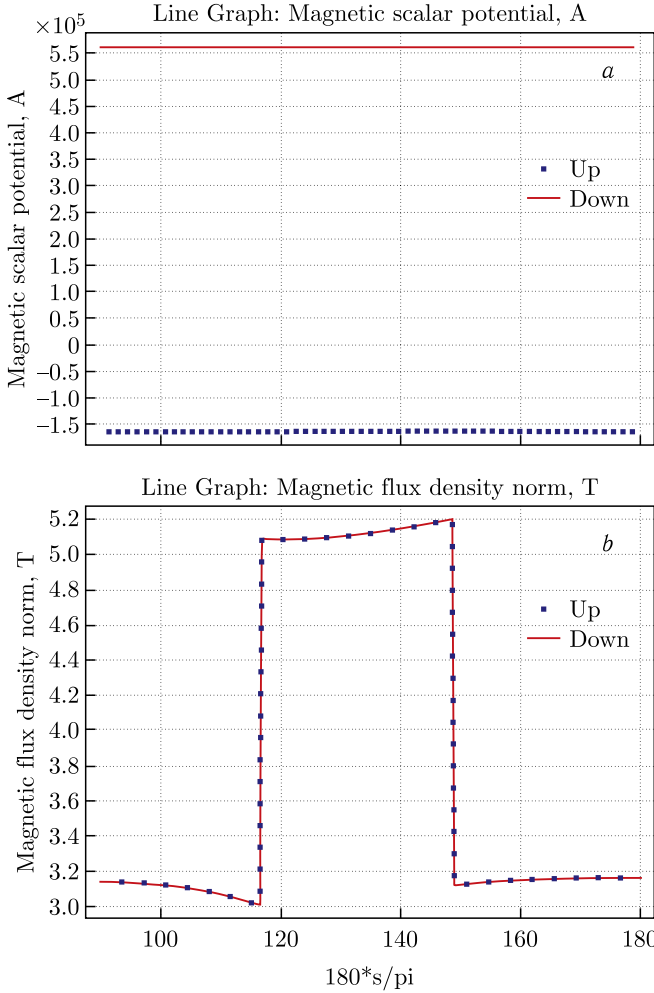


Fig. 3. Azimuthal distributions of the magnetic scalar potential (a) and the magnetic flux density norm (b) along up and down sides of the cut plane. The jump of the potential is exactly equal to the value of the applied coil current

Table 1. **Summary of formulations used for the Helmholtz coil**

Formulation	Element order	Number of FEs	Number of DOFs	Memory, GB Phys/Virtual	Time of computation
MVP&MSP	3/3	48 509	295 993	7.54/22.5	9 s
MVP	3	46 480	1 256 270	45.29/63.69	2 min 32 s

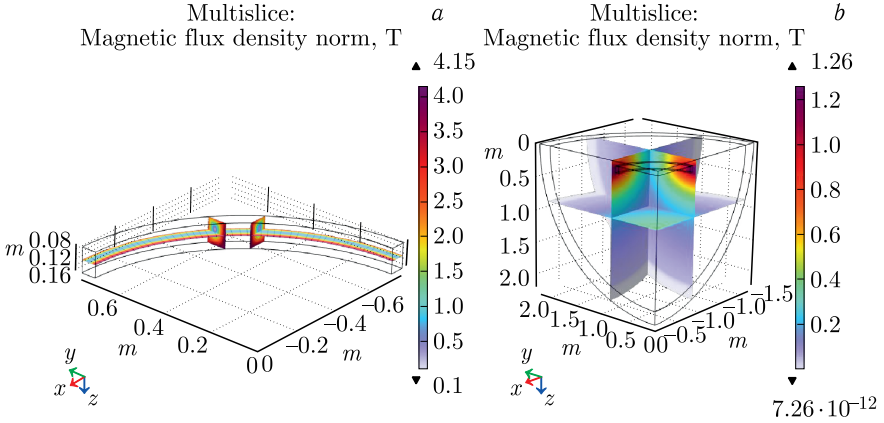


Fig. 4. Distributions of the magnetic flux density norm inside the coil (a) and the air (b) regions

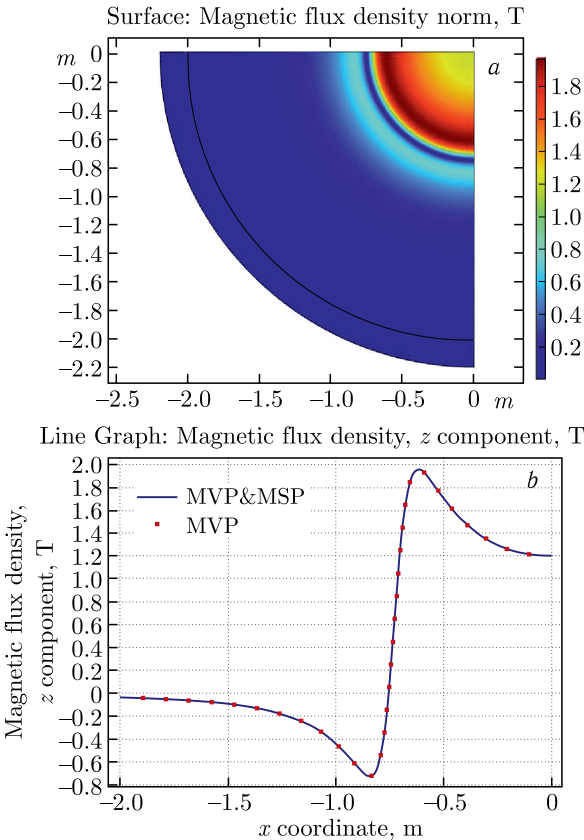


Fig. 5. Distributions of the magnetic flux density norm over the median plane (a) and the z component of the magnetic flux density along the radial direction (b). Solid line and points refer to calculations with MVP&MSP and MVP formulations, respectively

2.2. The Helmholtz Coil. The simulation results obtained for the finite-element modeling of the Helmholtz coil with the use of COMSOL software are shown in Figs. 4 and 5 and summarized in Table 1.

Both formulations produce excellent results in qualitative and quantitative agreement. As compared to the MVP formulation, the mixed formulation requires much less computational resources for the finite-element modeling of the Helmholtz coil. The reduction of DOFs amounts to a factor of 4.2, the RAM — to a factor of 6, and the time of computation — to a factor of 16.9 for relative error between the two formulations of 0.0001 T, or 1 G.

2.3. Dipole Magnet. Figures 6 and 7 present the simulation results obtained for the finite-element modeling of dipole magnet with the use of COMSOL software and summarized in Table 2. Both formulations produce the expected results in excellent qualitative and quantitative agreement. As compared to the MVP formulation, the mixed formulation requires much less computational resources for the finite-element modeling of dipole magnet. The reduction of DOFs amounts to a factor of 4.85, the RAM — to a factor of 10, and the time of computation — to a factor of 29.6 for relative error between the two formulations of 0.0003 T, or 3 G.

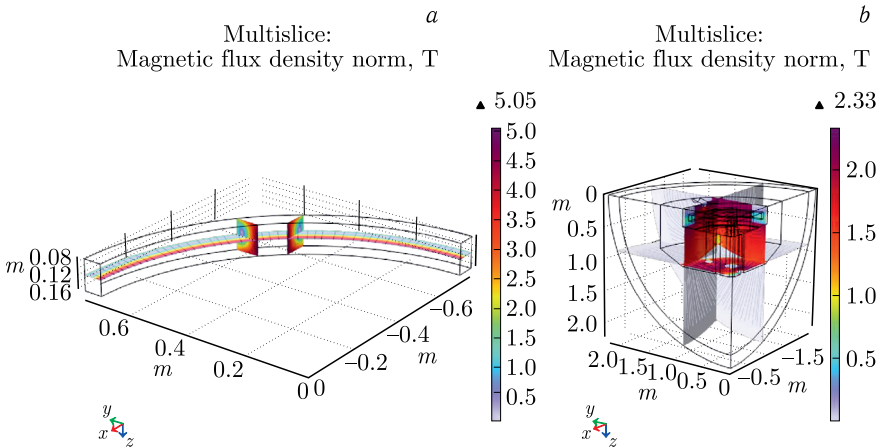


Fig. 6. Distributions of the magnetic flux density norm inside the coil (a) and the pole (b) regions

Table 2. Summary of formulations used for the dipole magnet

Formulation	Element order	Number of FEs	Number of DOFs	Memory, GB Phys/Virtual	Time of computation	Number of iterations
MVP&MSP	3/3	423 198	2 049 396	38.19/56.59	8 min 33 s	7
MVP	3	414 840	9 958 301	393.15/443.24	4 h 12 min 46 s	8

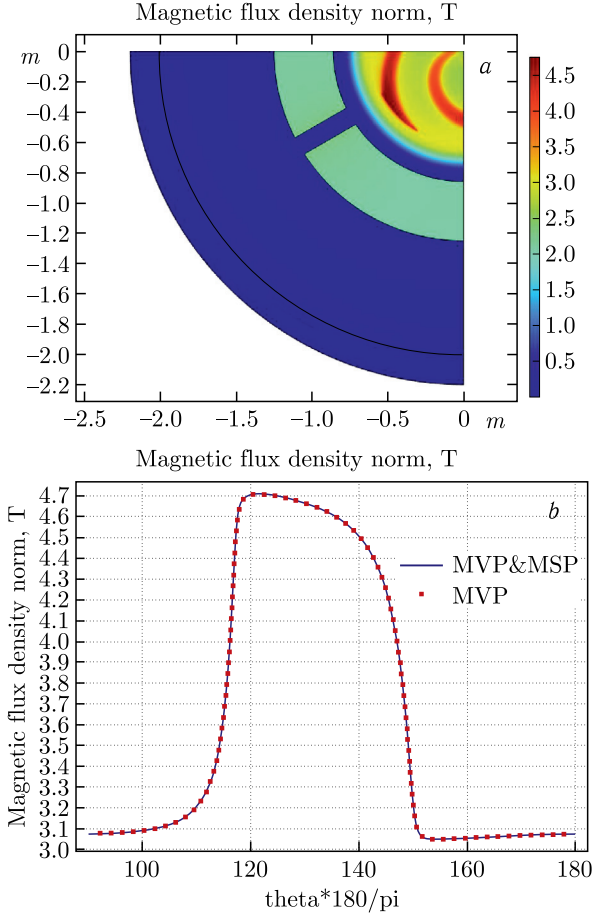


Fig. 7. Distributions of the magnetic flux density norm over the median plane (a) and along the azimuthal direction (b). Solid line and points refer to calculations with MVP&MSP and MVP formulations, respectively

CONCLUSIONS

In this paper, for the finite-element modeling of the large-scale magnetization problems in the presence of applied currents and highly nonlinear materials, we propose to use the combination of magnetic vector and total scalar potentials as an alternative to the well-known for its quality of calculation but computationally expensive vector potential formulation. The potentials are applied to conducting and nonconducting parts of the problem domain, respectively, and are coupled together across their common interfacing boundary. For nonconducting regions of the problem domain, the

thin cuts are constructed to ensure their simple connectedness and, therefore, the consistency of the mixed formulation. The numerical performance of the finite-element modeling in terms of combined potentials is assessed against the magnetic vector potential formulation for two magnetization models, the Helmholtz coil and the dipole magnet. We show that the mixed formulation can provide a substantial reduction in the computational cost as compared to its vector counterpart for a similar accuracy of both methods.

Acknowledgements. The computational support from HybriLIT Heterogeneous Computing Platform (MLIT JINR) is acknowledged.

REFERENCES

1. *De Gersem H., Garcia I. C., D'Angelo L. A. M., Schöps S.* Magnetodynamic Finite-Element Simulation of Accelerator Magnets // Proc. of the CERN Accelerator School on Numerical Methods for Analysis, Design and Modelling of Particle Accelerators. Thessaloniki, Greece, Nov. 11–23, 2018.
2. *Cheroyakov A.* Finite-Element Modelling of Magnetic Fields for Superconducting Magnets with Magnetic Vector and Total Scalar Potentials Using COMSOL Multiphysics® // Int. J. Engin. Syst. Model. Simul. 2022. V. 13. P. 117–133.
3. *Kleeven W., Zarembo S.* Cyclotrons: Magnetic Design and Beam Dynamics. physics.med-ph/arXiv:1804.08961. 2018.
4. *Karamysheva G. et al.* Compact Superconducting Cyclotron SC200 for Proton Therapy // Proc. of the 21st Intern. Conf. on Cyclotrons and Their Applications. Zurich, Switzerland, 2016. P. 371–373.
5. *Kuczmann M.* Potential Formulations in Magnetics Applying Finite Element Method: Lecture Notes. Győr, Hungary: Istvan Univ., 2009.
6. *Biro O., Preis K., Richter K.R.* On the Use of the Magnetic Vector Potential in the Nodal and Edge Finite Element Analysis of 3D Magnetostatic Problems // IEEE Trans. Magn. 1996. V. 32. P. 651–654.
7. *Biro O., Preis K.* On the Use of the Magnetic Vector Potential in the Finite Element Analysis of Three-Dimensional Eddy Currents // IEEE Trans. Magn. 1989. V. 25. P. 3145–3159.
8. *Guerin C., Tanneau G., Meunier G., Brunotte X., Albertini J.B.* Three-Dimensional Magnetostatic Finite Elements for Gaps, and Iron Shells Using Magnetic Scalar Potentials // IEEE Trans. Magn. 1994. V. 30. P. 2885–2888.
9. *Gross P.W., Kotiuga P.R.* Electromagnetic Theory and Computation: A Topological Approach. Cambridge: Cambridge Univ. Press, 2004.
10. *Rodger D., Eastham J.* Multiply Connected Regions in the $A - \psi$ Three-Dimensional Eddy-Current Formulation // IEE Proc. A (Physical Science, Measurement and Instrumentation, Management and Education, Reviews). 1987. V. 134. P. 58.
11. *Stockrahm A., Lahtinen V., Kangas J.J.J., Kotiuga P.R.* Cuts for 3-D Magnetic Scalar Potentials: Visualizing Unintuitive Surfaces Arising from Trivial Knots. physics.comp-ph/arXiv:1902.01124v2. 2019.
12. *Cheroyakov A.* Comparison of Magnetic Vector and Total Scalar Potential Formulations for Finite-Element Modeling of Dipole Magnet with COMSOL Multiphysics. physics.comp-ph/arXiv:2107.01957. 2021.

13. *Crawford C.B.* The Physical Meaning of the Magnetic Scalar Potential and Its Use in the Design of Hermetic Electromagnetic Coil // *Rev. Sci. Instrum.* 2021. V. 92. P. 1–8.
14. *Jackson J.D.* *Classical Electrodynamics.* 3rd ed. New York: John Wiley & Sons, 1998.
15. *Bergström R.* Least-Squares Finite Element Methods for Electromagnetic Applications. Preprint 2000-005. Göteborg, Sweden: Chalmers Univ. of Technology, 2000.
16. *Volakis J.L., Chatterjee A., Kempel L.C.* *Finite Element Method for Electromagnetics.* New York: Wiley-IEEE, 1998.
17. *Monk P.* *Finite Element Method for Maxwell's Equations.* Oxford: Clarendon Press, 2003.
18. *Bedrosian G.* High-Performance Computing for Finite Element Methods in Low-Frequency Electromagnetics // *Prog. Electromagn. Res.* 1993. V. 7. P. 57–110.
19. *Mur G.* Edge Elements, Their Advantages, and Their Disadvantages // *IEEE Trans. Magn.* 1994. V. 30. P. 3552–3557.
20. *Creuse E., Dular P., Nicaise S.* About Gauge Conditions Arising in Finite Element Magnetostatic Problems // *Comput. Math. Appl.* 2019. V. 77. P. 1563–1582.
21. *Boffi D., Gastaldi L.* Edge Finite Elements for the Approximation of Maxwell Resolvent Operator // *Math. Model. Numeric. Anal.* 2002. V. 36. P. 293–305.
22. *Tagami D.* Efficient Numerical Computations on Large Scale Electromagnetic Field Problems Using an Iterative Domain Decomposition Method // *Lecture Notes Ser.* 2012. V. 39. P. 96–101.
23. *Kikuchi F.* Mixed Formulations for Finite Element Analysis of Magnetostatic and Electrostatic Problems // *Japan J. Indust. Appl. Math.* 1989. V. 6. P. 209–221.
24. *Kamireddy D., Nandy A.* A Novel Conversion Technique from Nodal to Edge Finite Element Data Structure for Electromagnetic Analysis. [math.NA/arXiv:2103.15379v1](https://arxiv.org/abs/2103.15379v1). 2021.
25. COMSOL Multiphysics®. AC/DC Module, User's Guide. COMSOL AB, Stockholm, 2018.

Received on July 24, 2023.

Редактор *В. В. Булатова*

Подписано в печать 4.10.2023.

Формат 60 × 90/16. Бумага офсетная. Печать цифровая.

Усл. печ. л. 1,18. Уч.-изд. л. 1,28. Тираж 105 экз. Заказ № 60738.

Издательский отдел Объединенного института ядерных исследований
141980, г. Дубна, Московская обл., ул. Жолио-Кюри, 6.

E-mail: publish@jinr.ru

www.jinr.ru/publish/